Science Advances

AAAS

advances.sciencemag.org/cgi/content/full/2/2/e1501162/DC1

Supplementary Materials for

Miniature high-throughput chemosensing of yield, ee, and absolute configuration from crude reaction mixtures

Keith W. Bentley, Peng Zhang, Christian Wolf

Published 12 February 2016, *Sci. Adv.* **2**, e11501162 (2016)
DOI: 10.1126/sciadv.1501162

The PDF file includes:

1. General information

All reagents and solvents were commercially available and used without further purification. Reactions were carried out under inert atmosphere and anhydrous conditions. Flash chromatography was performed on silica gel, particle size 40-63 μm. NMR spectra were obtained at 400 MHz (^{1}H-NMR) and 100 MHz (^{13}C-NMR) using $CDCl_3$ as solvent and TMS as reference.

2. Synthetic procedures

Scheme S1. General synthesis of 1.

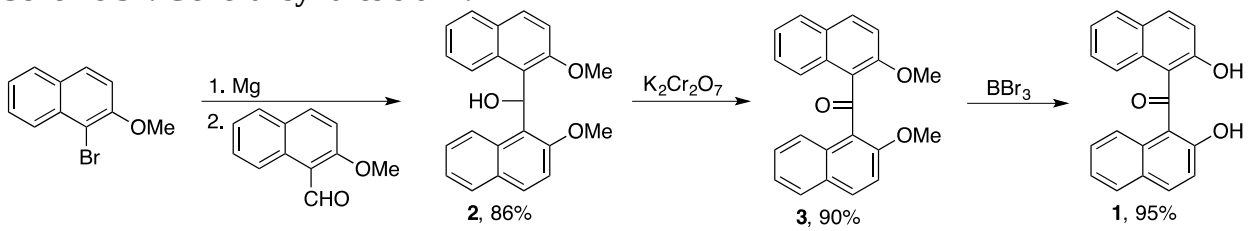

1,1-Bis(2-methoxy-1-naphthyl)methanol (2)
A solution of 2-methoxy-1-bromonaphthalene (500 mg, 2.1 mmol), Mg turnings (102 mg, 4.2 mmol) and I_2 (32 mg, 0.13 mmol) in 6 mL THF was stirred at reflux for 2 hours. The reaction mixture was cooled to 0 °C and 2-methoxy-1-naphthaldehyde (432 mg, 2.3 mmol, 0.8 M in THF) was added dropwise. The reaction mixture was then stirred at room temperature for 2 hours, quenched with NH_4Cl and extracted with CH_2Cl_2. The combined organic layers were dried over $MgSO_4$ and concentrated in vacuo. Purification by flash chromatography on silica gel (hexanes:EtOAc 4:1) afforded 625 mg (1.8 mmol, 86%) of a white solid.
^{1}H NMR δ = 3.65 (s, 6H), 6.01 (d, *J* = 8.7 Hz, 1H), 7.28-7.42 (m, 6H), 7.75 (dd, *J* = 8.8 Hz, 7.6 Hz, 4H), 8.10 (d, 8.4 Hz, 2H). ^{13}C NMR δ =57.1, 68.5, 115.0, 123.5, 123.6, 125.5, 126.8, 128.6, 129.6, 129.7, 132.4, 155.3. Anal. Calcd. $C_{23}H_{20}O_3$: C, 80.21; H, 5.85. Found: C, 80.51; H, 6.14.

Bis(2-methoxy-1-naphthyl)ketone (3)
A solution of **2** (370 mg, 1.1 mmol) and $K_2Cr_2O_7$ (348 mg, 1.2 mmol) in 8 mL DMF was stirred at 100 °C for 12 hours. The mixture was allowed to cool to room temperature, quenched with water, and extracted with CH_2Cl_2. The combined organic layers were dried over $MgSO_4$ and concentrated in vacuo. The residue was washed with hexanes to give 326 mg (1.0 mmol, 90%) of a light brown solid.
^{1}H NMR δ = 3.37 (s, 6H), 7.15 (d, *J* = 9.0 Hz, 2H), 7.40 (dd, *J* = 7.2 Hz, 7.2 Hz, 2H), 7.51 (dd, *J* = 7.3 Hz, 7.3 Hz, 2H), 7.81 (d, *J* = 8.2 Hz, 2H), 7.88 (d, *J* = 9.0 Hz, 2H), 8.18 (d, *J* = 8.7 Hz, 2H). ^{13}C NMR δ =56.7, 113.9, 124.0, 125.1, 127.2, 127.4, 127.9, 129.2, 131.7, 131.9, 155.6, 199.8. Anal. Calcd. $C_{23}H_{18}O_3$: C, 80.68; H, 5.30. Found: C, 80.67: H, 5.59.

Bis(2-hydroxy-1-naphthyl)ketone (1)
A solution of **3** (320 mg, 0.9 mmol) and BBr_3 (1M in CH_2Cl_2, 5.6 mL, 5.6 mmol) in 5 mL CH_2Cl_2 was stirred at 0 °C for 30 minutes. The reaction mixture was quenched with H_2O and extracted with CH_2Cl_2. The combined organic layers were dried over $MgSO_4$ and concentrated

in vacuo. Purification by flash chromatography (hexanes:EtOAc 3:1) afforded 275 mg (0.88 mmol, 95%) of a yellow solid.
^{1}H NMR δ = 6.83 (dd, *J* = 8.4 Hz, 7.1 Hz, 2H), 7.04 (d, *J* = 8.6 Hz, 2H), 7.09 (dd, *J* = 8.6 Hz, 7.1 Hz, 2H), 7.28 (d, *J* = 9.0 Hz, 2H), 7.64 (d, *J* = 9.0 Hz, 2H), 7.94 (d, *J* = 8.4 Hz, 2H), 10.84 (s, 2H). ^{13}C NMR δ =117.4, 119.3, 123.9, 124.1, 127.3, 128.3, 128.4, 131.3, 136.7, 160.1, 200.4. Anal. Calcd. $C_{21}H_{14}O_3$: C, 80.24; H, 4.49. Found: C, 80.16; H, 4.66.

Figure S1. ^{1}H and ^{13}C NMR Spectra of 2 in $CDCl_3$

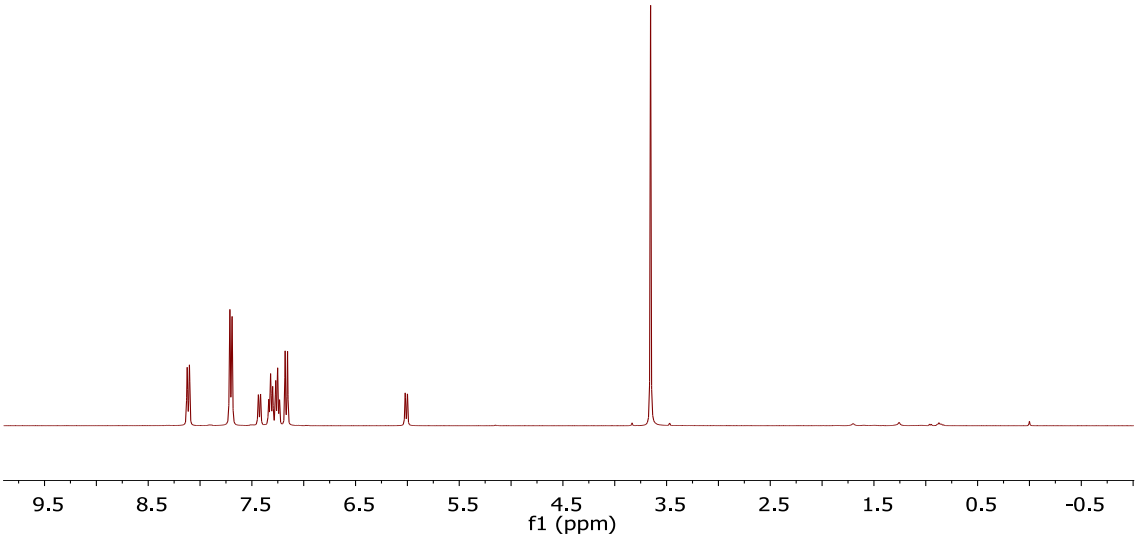

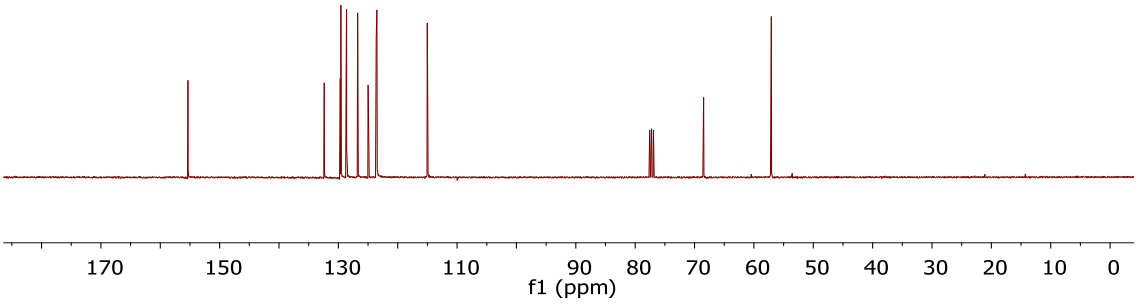

Figure S2. ^{1}H and ^{13}C NMR Spectra of 3 in $CDCl_3$

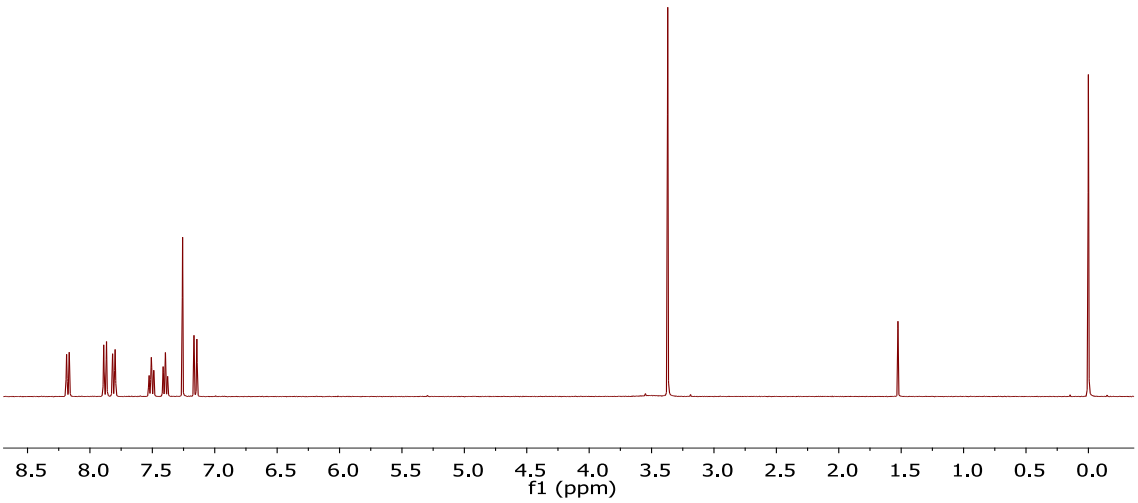

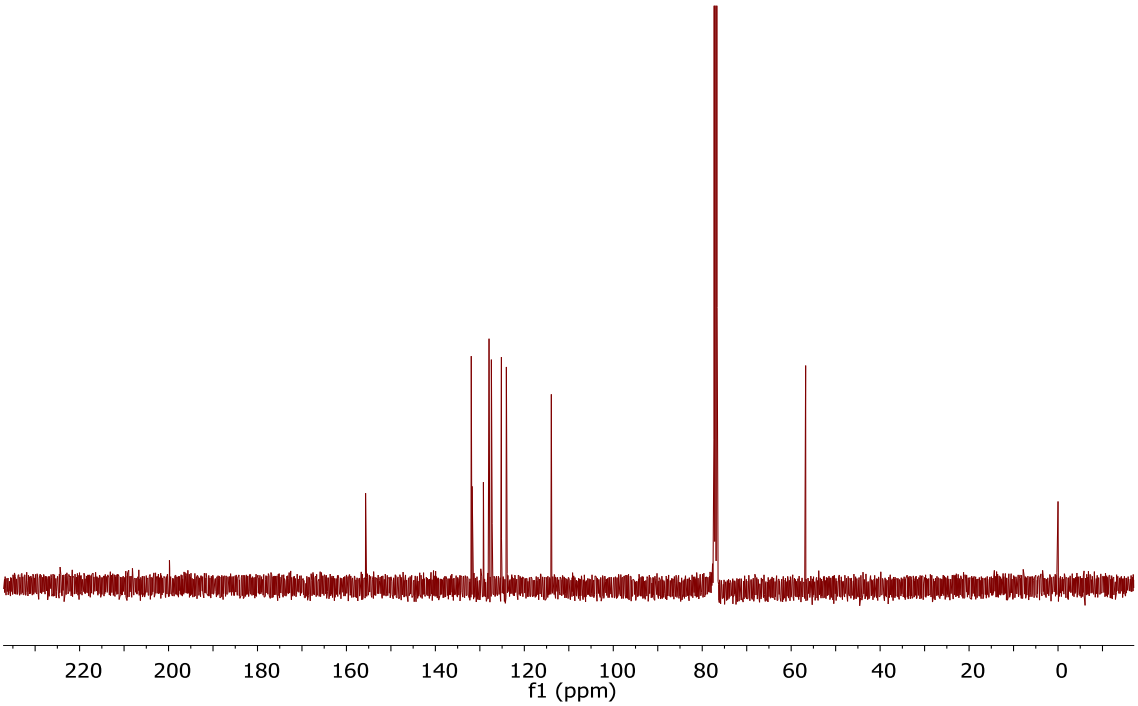

Figure S3. ^{1}H and ^{13}C NMR Spectra of 1 in $CDCl_3$

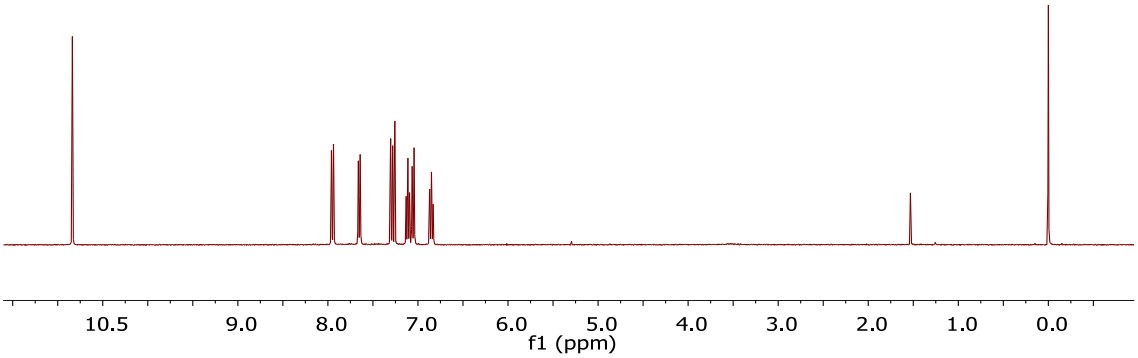

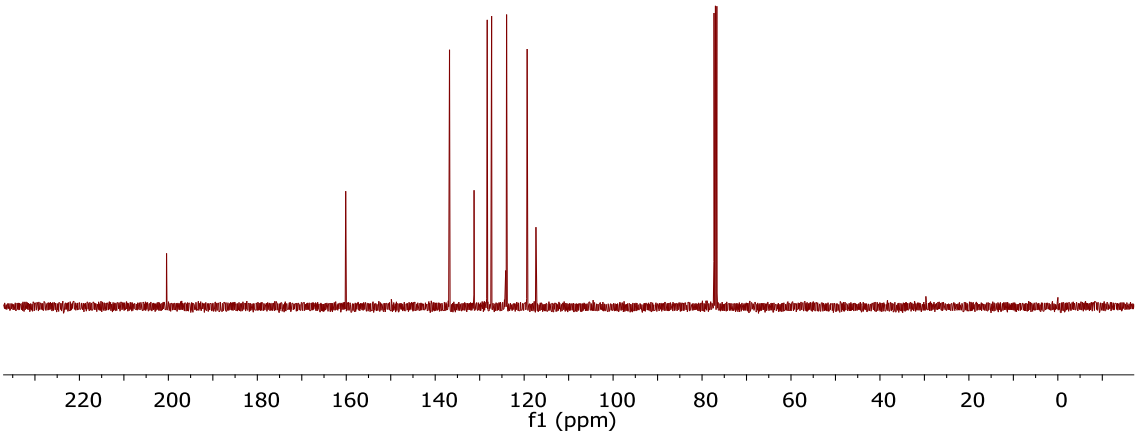

3. Enantioselective sensing experiments

3.1. Substrate scope

Bis(2-hydroxy-1-naphthyl)ketone, **1**, was treated with Et_2Zn, Me_3Al, or $Ti(O\textit{i}\text{-}Pr)_4$ using THF or DMSO as solvent. To the corresponding metal complexes were added substrates **4-18** (Zn), **19-24** (Al) and **25-29** (Ti), and the chiroptical properties of the resulting adducts were analyzed by CD spectroscopy as described below. The analytes are not CD active in the absence of **1** under the same conditions.

Figure S4. Structures of substrates 4-29 (only one enantiomer shown).

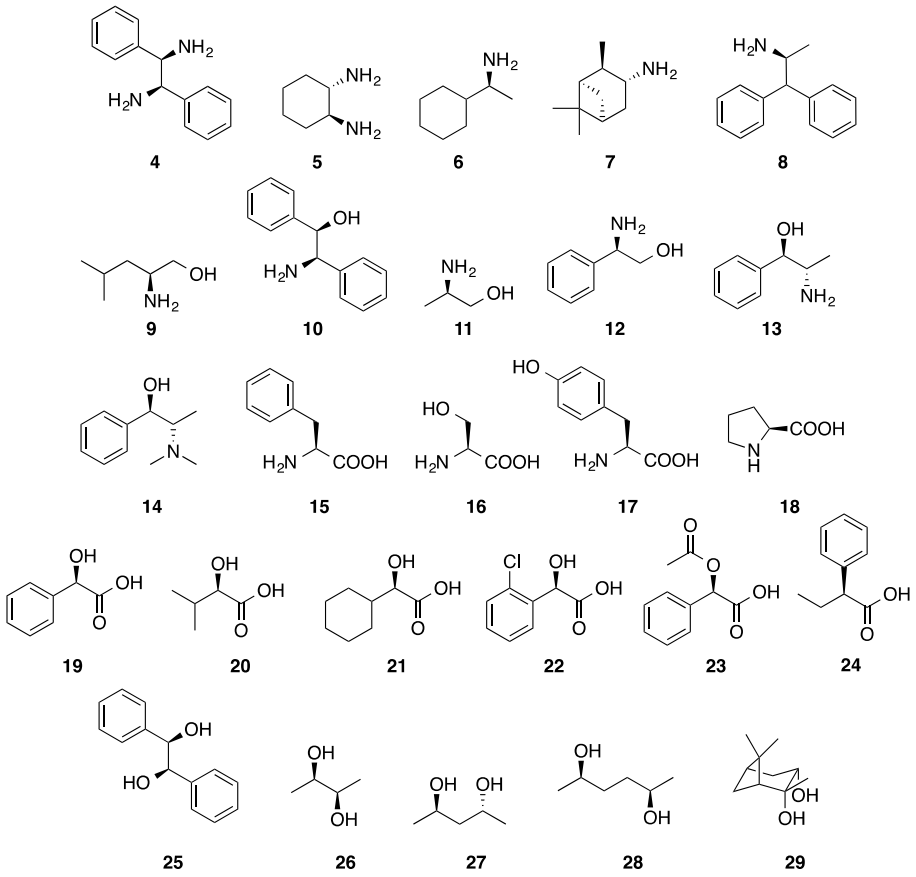

3.2. Amines and amino alcohols

A stock solution of **1** (0.01 M) in anhydrous THF was prepared and 500 μL portions were placed into 4 mL vials containing one equivalent of diamines **4** and **5**, 2 equivalents of amines **6-8** (0.005 mmol) or one equivalent of amino alcohols **9-14**. To each vial was then added Et_2Zn (5 μL, 0.005 mmol, 1M in hexanes), causing an immediate color change from yellow to orange. The mixtures were stirred for 5 minutes and CD analysis was conducted by adding 30 μL of the mixtures into 2 mL of anhydrous diethyl ether to obtain a sample concentration of 1.13×10^{-4} M. The CD spectra were collected with a standard sensitivity of 100 mdeg, a data pitch of 0.5 nm, a

bandwidth of 1 nm, a scanning speed of 500 nm s^{-1} and a response of 0.5 s using a quartz cuvette (1 cm path length). The data were baseline corrected and smoothed using a binomial equation.

Figure S5. Circular dichroism response of the zinc complex of 1 to chiral diamines, amines and amino alcohols.

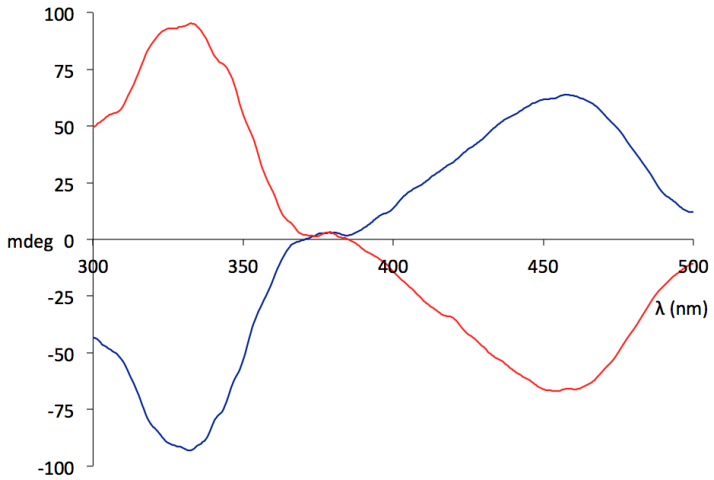

CD Spectra obtained using **1** and (1*R*,2*R*)-**4** (blue) and (1*S*,2*S*)-**4** (red).

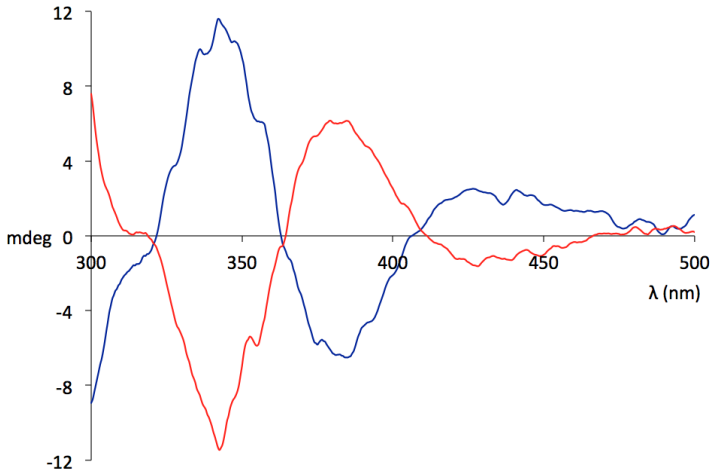

CD Spectra obtained using **1** and (1*R*,2*S*)-**5** (blue) and (1*S*,2*R*)-**5** (red).

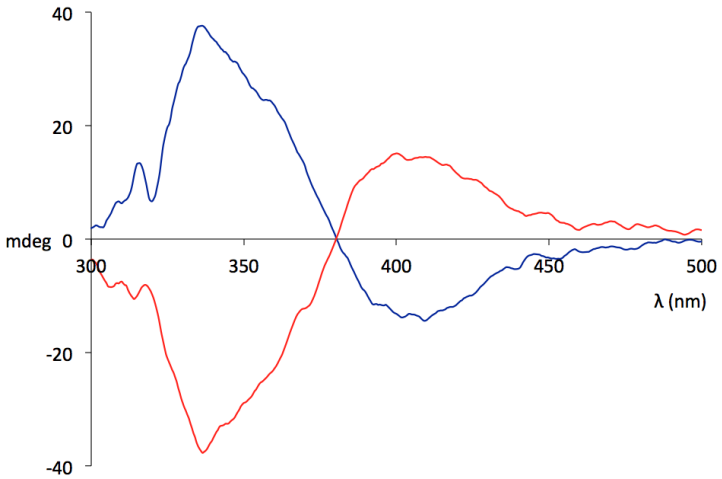

CD Spectra obtained using **1** and (*R*)-**6** (blue) and (*S*)-**6** (red).

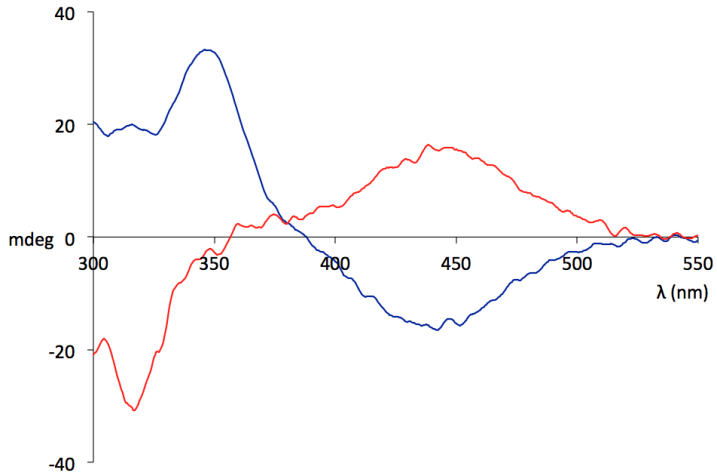

CD Spectra obtained using **1** and (1*R*,2*R*,3*R*,5*S*)-**7** (blue) and (1*S*,2*S*,3*S*,5*R*)-**7** (red).

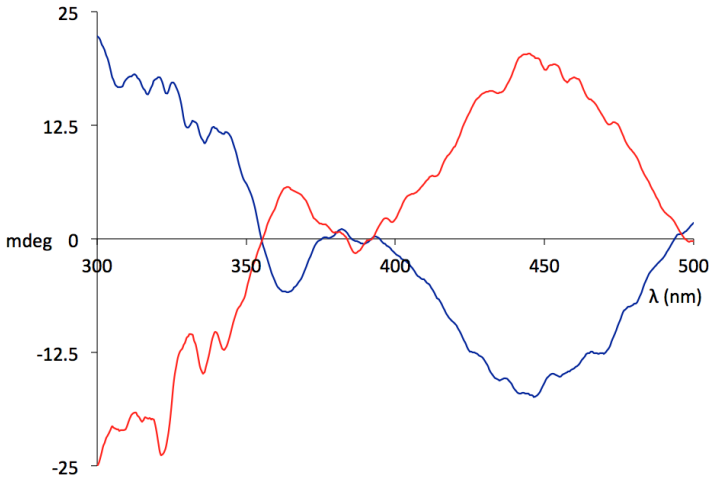

CD Spectra obtained using **1** and (*R*)-**8** (blue) and (*S*)-**8** (red).

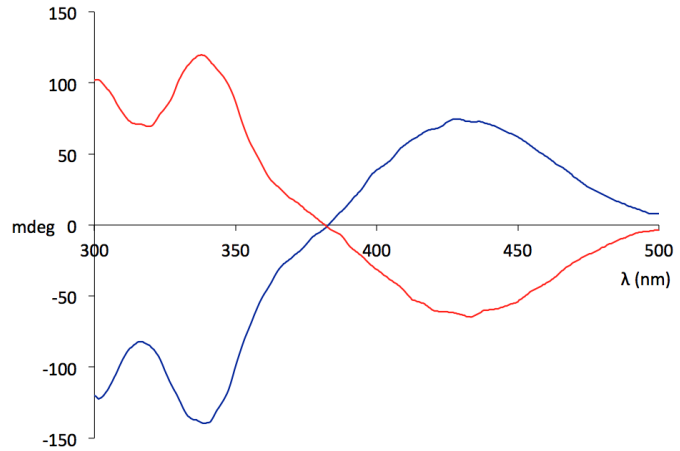

CD Spectra obtained using **1** and (*R*)-**9 (**blue) and (*S*)-**9** (red).

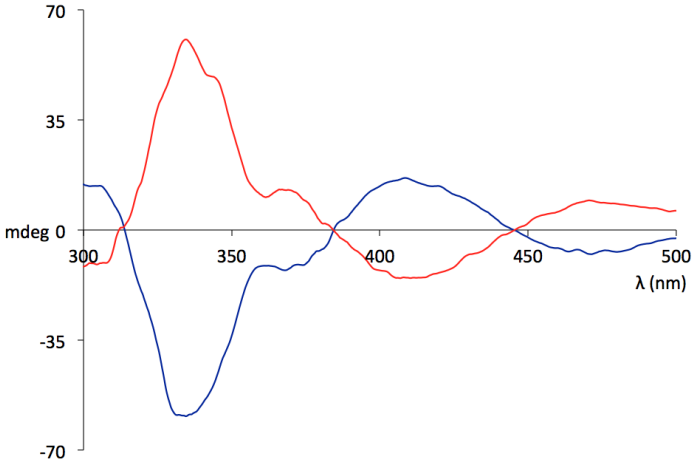

CD Spectra obtained using **1** and (1*S*,2*R*)-**10** (blue) and (1*R*,2*S*)-**10** (red).

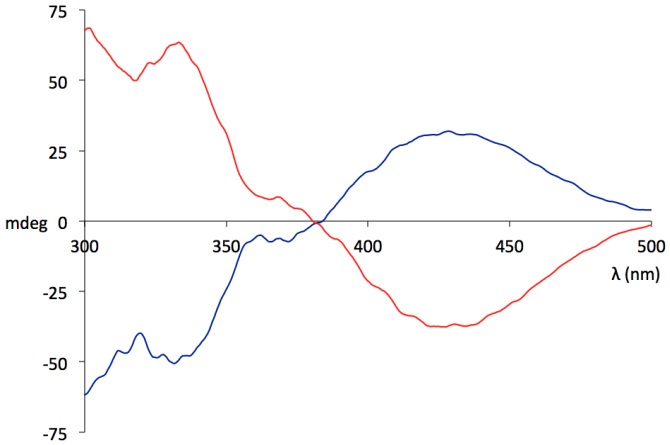

CD Spectra obtained using **1** and (*R*)-**11** (blue) and (*S*)-**11** (red).

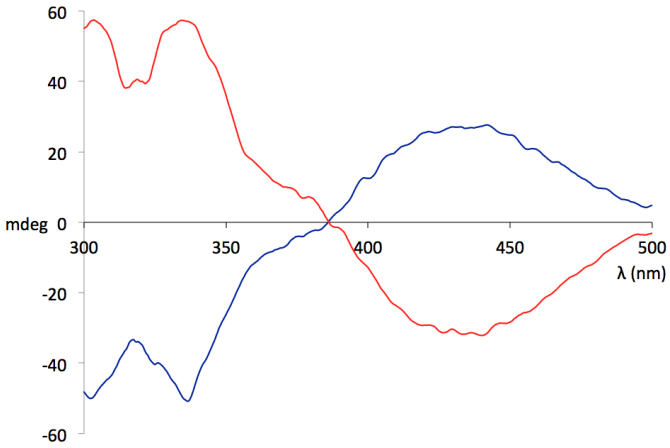

CD Spectra obtained using **1** and (*R*)-**12** (blue) and (*S*)-**12** (red).

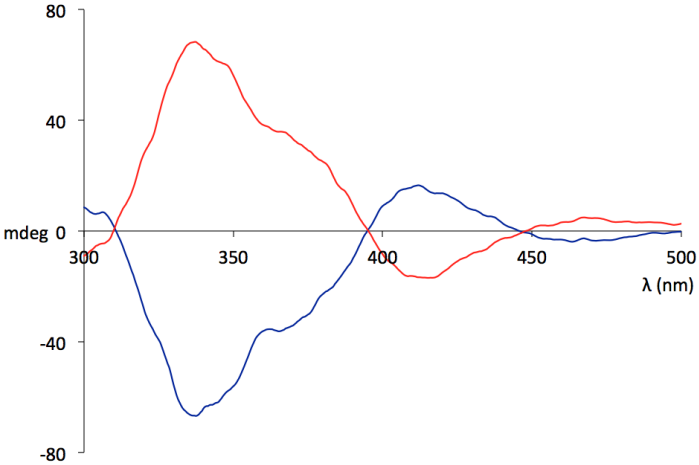

CD Spectra obtained using **1** and (1*S*,2*R*)-**13** (blue) and (1*R*,2*S*)-**13** (red).

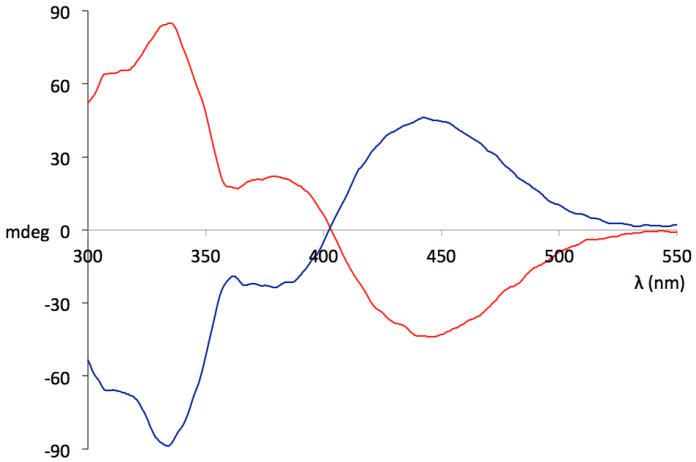

CD Spectra obtained using **1** and (1*S*,2*R*)-**14** (blue) and (1*R*,2*S*)-**14** (red).

3.3. Amino acids

A stock solution of **1** (0.01 M) in anhydrous DMSO was prepared and 500 µL portions were placed into 4 mL vials containing one equivalent of amino acids **15-18**. To each vial was then added Et_2Zn (5 µL, 0.005 mmol, 1M in hexanes), causing an immediate color change from yellow to orange. The mixtures were stirred for 5 minutes and CD analyses were conducted as described above.

Figure S6. Circular dichroism response of the zinc complex of 1 to chiral amino acids.

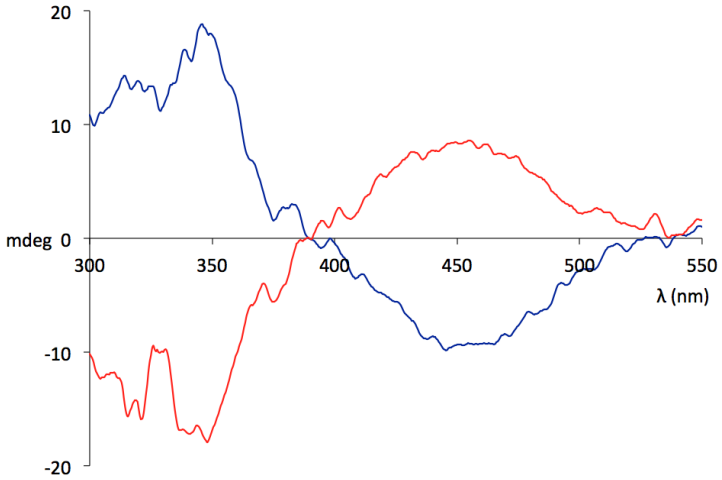

CD Spectra obtained using **1** and (*R*)-**15** (blue) and (*S*)-**15** (red).

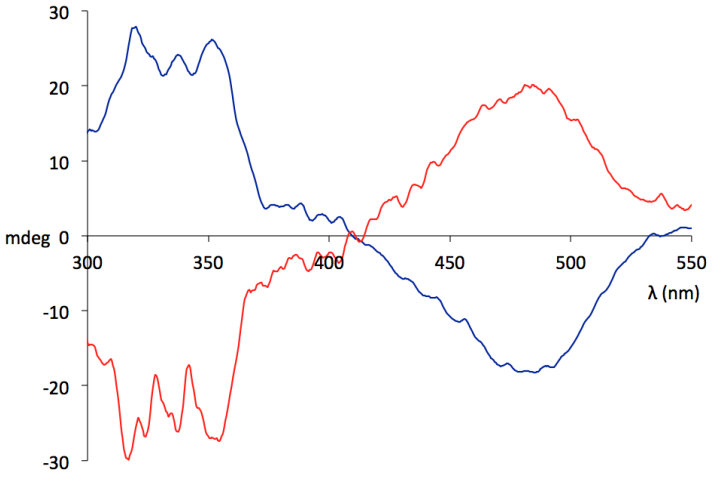

CD Spectra obtained using **1** and (*R*)-**16** (blue) and (*S*)-**16** (red).

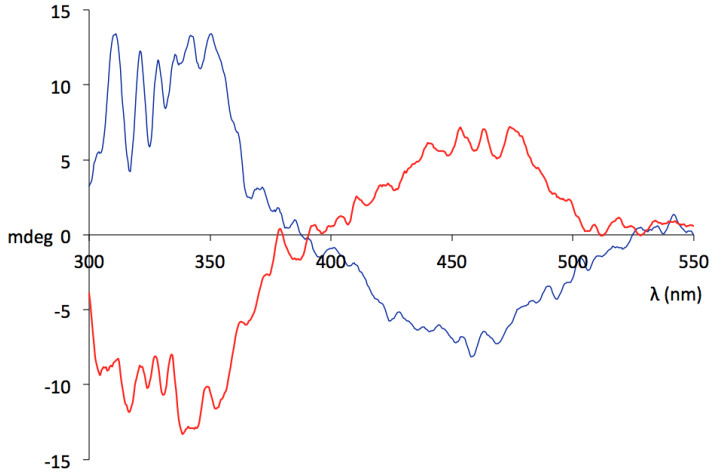

CD Spectra obtained using **1** and (*R*)-**17** (blue) and (*S*)-**17** (red).

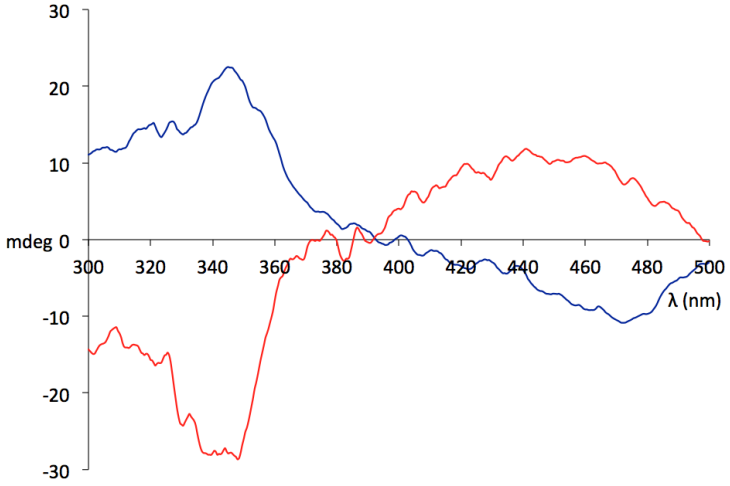

CD Spectra obtained using **1** and (*R*)-**18** (blue) and (*S*)-**18** (red).

3.4. Carboxylic acids

A stock solution of **1** (0.01 M) in anhydrous THF was prepared and 500 μL portions were placed into 4 mL vials containing one equivalent of carboxylic acids **19**-**24**. To each vial was then added Me_3Al (2.5 μL, 0.005 mmol, 2M in hexanes), causing an immediate color change from yellow to red. Et_3N (0.7 μL, 0.005 mmol) was also added to solutions containing substrates **19**-**22**. The mixtures were stirred for 5 minutes and CD analyses were conducted as described above.

Figure S7. Circular dichroism response of the aluminum complex of 1 to carboxylic acids.

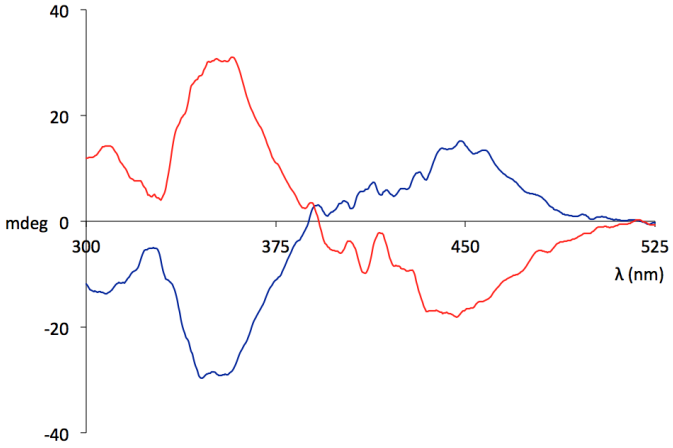

CD Spectra obtained using **1** and (*R*)-**19** (blue) and (*S*)-**19** (red).

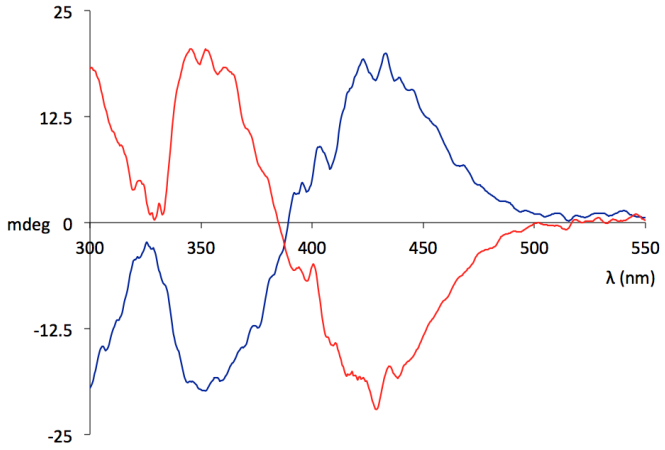

CD Spectra obtained using **1** and (*R*)-**20** (blue) and (*S*)-**20** (red).

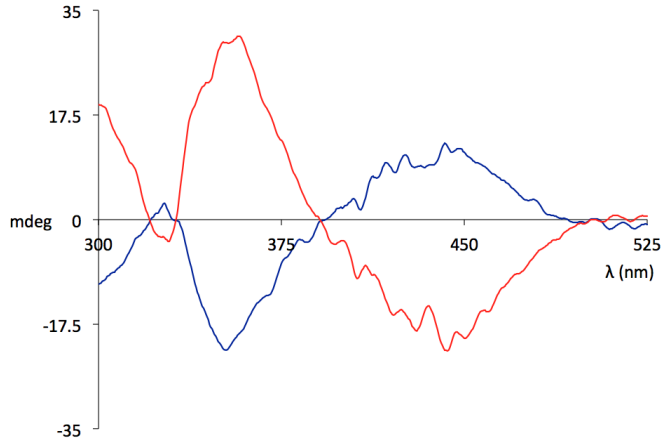

CD Spectra obtained using **1** and (*R*)-**21** (blue) and (*S*)-**21** (red).

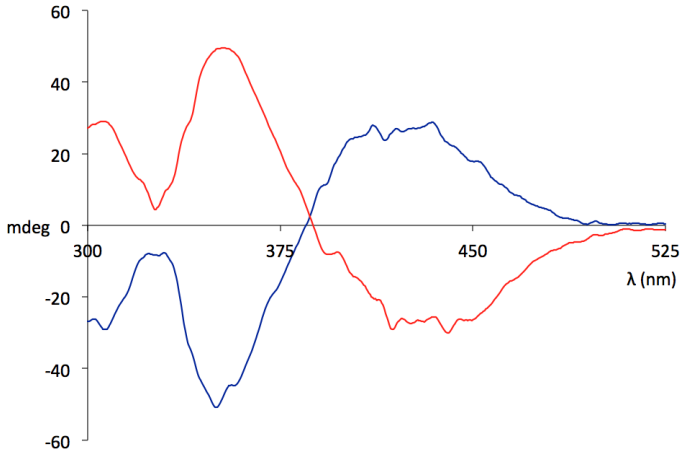

CD Spectra obtained using **1** and (*R*)-**22** (blue) and (*S*)-**22** (red).

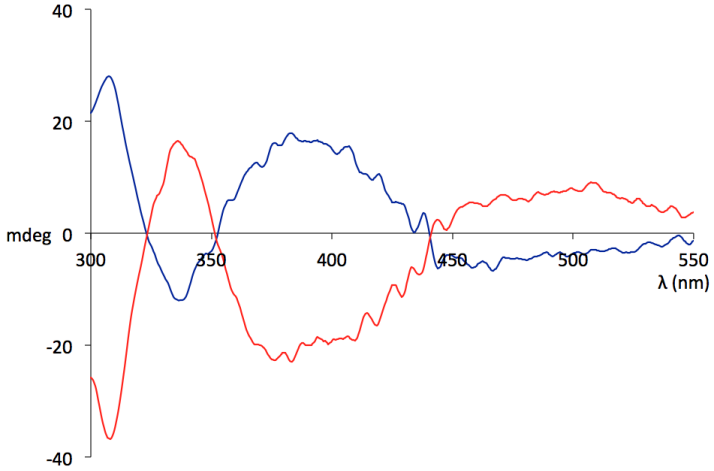

CD Spectra obtained using **1** and (*R*)-**23** (blue) and (*S*)-**23** (red).

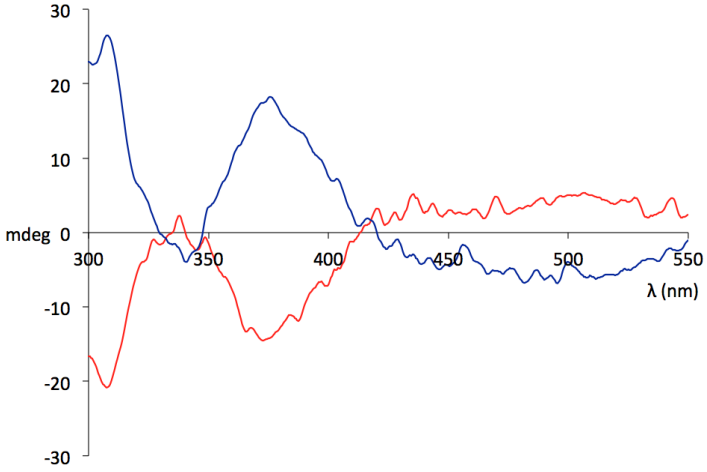

CD Spectra obtained using **1** and (*R*)-**24** (blue) and (*S*)-**24** (red).

3.5. Diols

A stock solution of **1** (0.01 M) in anhydrous THF was prepared and 500 μL portions were placed into 4 mL vials containing a diol **25**-**29** (0.005 mmol). To each vial was then added Ti(O*i*-Pr)$_4$ (1.48 μL, 0.005 mmol), and an immediate color change from yellow to red was observed. The solutions were stirred for 10 minutes and CD analyses were conducted as described above.

Figure S8. Circular dichroism response of the titanium complex of 1 to chiral diols.

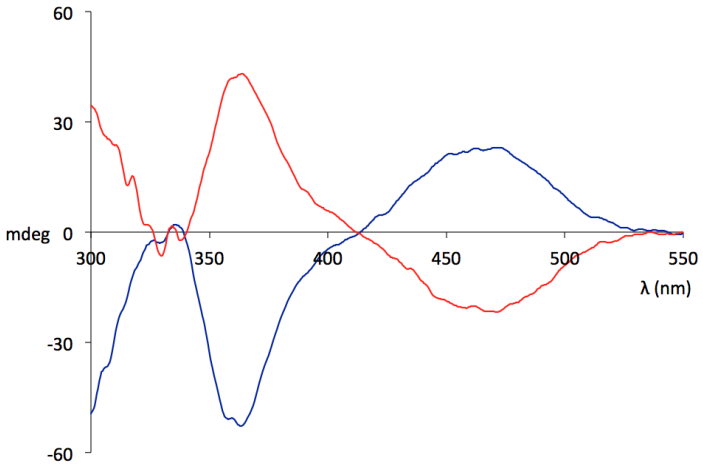

CD Spectra obtained using **1** and (1*R*,2*R*)-**25** (blue) and (1*S*,2*S*)-**25** (red).

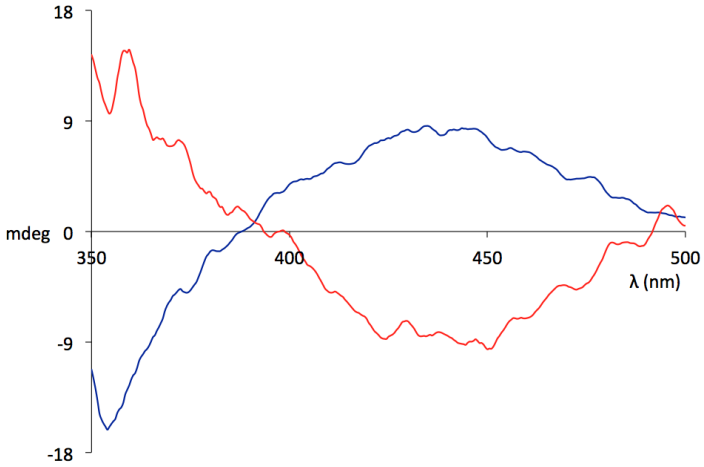

CD Spectra obtained using **1** and (2*R*,3*R*)-**26** (blue) and (2*S*,3*S*)-**26** (red).

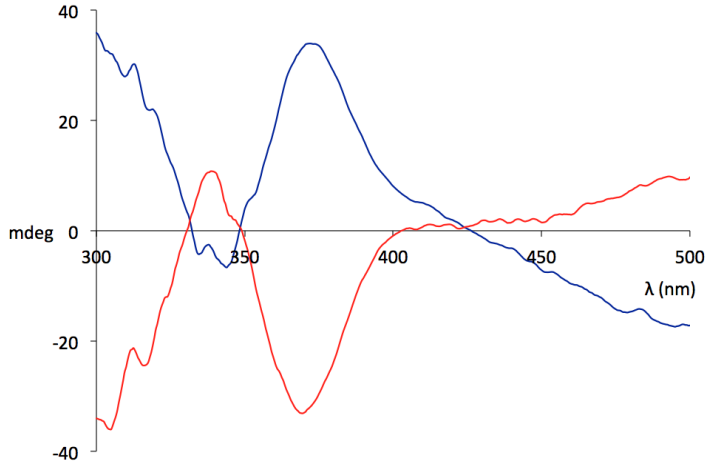

CD Spectra obtained using **1** and (2*R*,4*R*)-**27** (blue) and (2*S*,4*S*)-**27** (red).

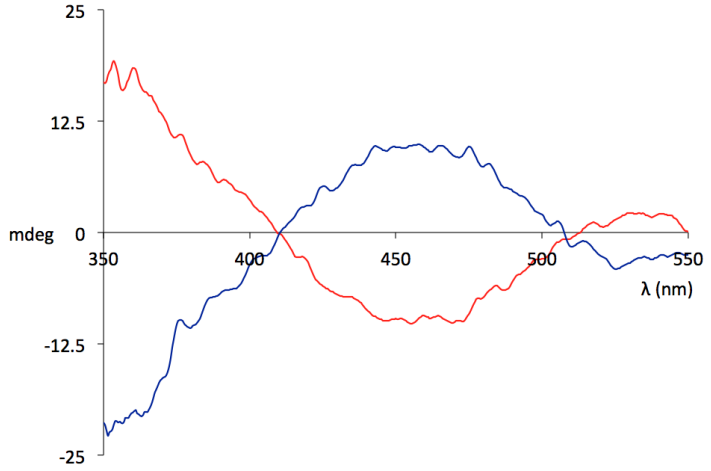

CD Spectra obtained using **1** and (2*R*,5*R*)-**28** (blue) and (2*S*,5*S*)-**28** (red).

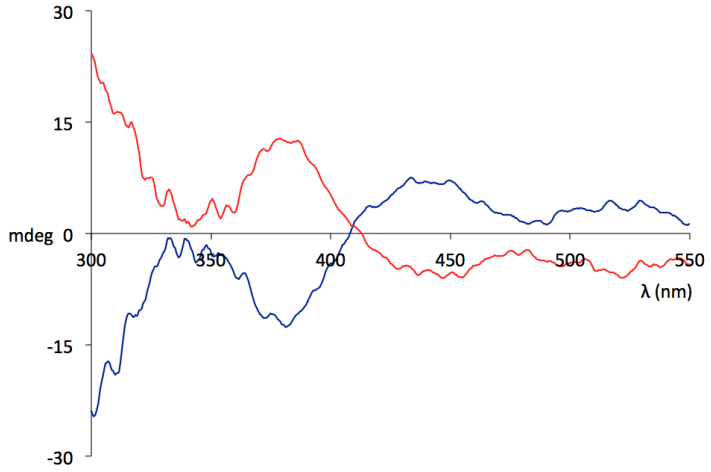

CD Spectra obtained using **1** and (1*R*,2*R*,3*S*,5*R*)-**29** (blue) and (1*S*,2*S*,3*R*,5*S*)-**29** (red).

3.6. Comparison of the CD effects of 1 with mandelic acid using Me_3Al and $B(OMe)_3$

A solution of **1**, Me_3Al, and **19** was prepared as described above. A separate solution of **1**, **19** and $B(OMe)_3$ (0.56 μL, 0.005 mmol) in $CHCl_3$ was also prepared, and the CD responses of the corresponding complexes were collected as previously described.

Figure S9. CD Spectra obtained from 1, (*S*)-19 and Me_3Al (solid red) and from 1, (*S*)-19 and $B(OMe)_3$ (dashed red).

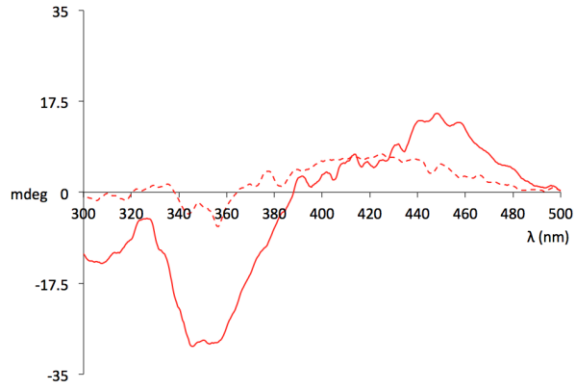

4. Quantitative ee and concentration analysis

4.1. Ee determination of *N*-methylephedrine 14

CD responses of the Zn complex prepared with **1** and **14** at varying ee were recorded. Solutions containing **1** (0.00375 M in THF) and **14** (0.07 M in THF) with varying enantiomeric composition (+100, +80, +60, +40, +20, 0, -20, -40, -60, -80, -100 ee) were prepared. To these solutions was added Et_2Zn (1.3 μL, 0.0013 mmol, 1M in hexanes). After 5 minutes, CD analysis was carried out as described above at 1.13 x 10^{-4} M in anhydrous diethyl ether. The Cotton effect amplitudes at 338, 385, and 445 nm were plotted against the enantiomeric excess of **14**.

Figure S10. CD Spectra of the Zn complex obtained with 1 and scalemic samples of 14.

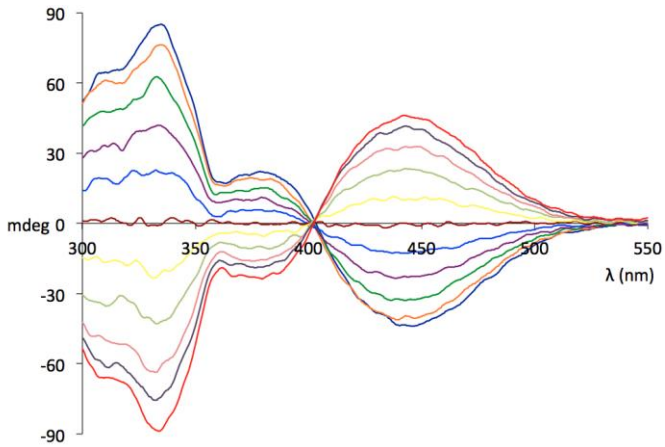

Figure S11. Exponential relationship between the CD amplitudes at 338 nm (blue), 385 nm (red), and 445 nm (green) and the enantiomeric excess of 14.

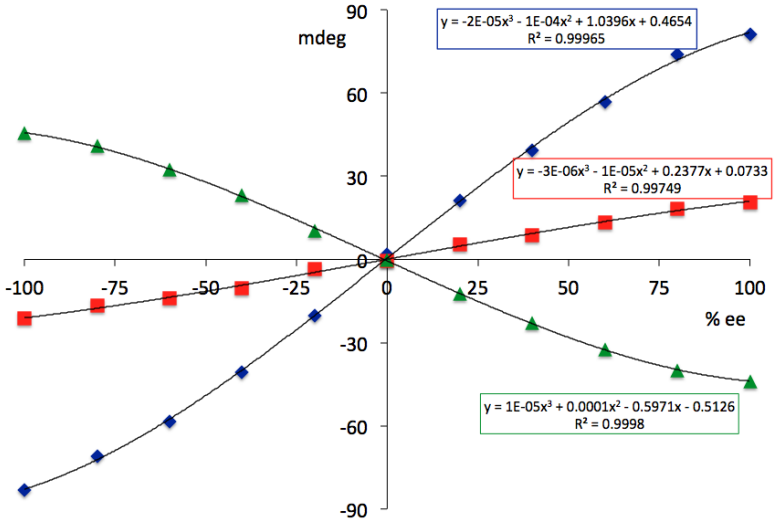

Six scalemic samples of **14** were prepared and subjected to CD analysis with **1** and Et_2Zn as described above. The enantiomeric excess of these samples was determined using the regression equations obtained above and the CD amplitudes measured at 338, 385, and 445 nm.

Table S1. Ee determination of *N*-methylephedrine.

Actual % ee (*R*)	Calculated % ee at 338 nm (*R*)	Calculated % ee at 385 nm (*R*)	Calculated % ee at 445 nm (*R*)	Average % ee
87.0	85.4	89.5	82.6	85.8
76.0	78.5	79.3	76.7	78.2
12.0	12.4	11.6	11.7	11.9
-26.0	-27.2	-22.5	-24.3	-24.7
-68.0	-70.2	-65.3	-64.8	-66.8
-89.0	-90.6	-86.9	-84.2	-87.2

4.2. Determination of the concentration of 14

The change in the fluorescence of the complex between **1** and Et_2Zn upon addition of **14** was analyzed using samples containing various amounts of **14**. First, 350 μL solutions of **1** (0.00375 M in THF) were placed in 16 vials. To each vial was then transferred a solution of **14** (0.07 M in THF) in varying amounts (0, 10, 20, 30, 40, 50, 60, 70, 80, 90, 100, 120, 140, 160, 180 and 200 mol%). Et_2Zn (1.3 μL, 0.0013 mmol, 1M in hexanes) was added to each vial and the mixtures were allowed to react for 5 minutes. Fluorescence spectra were collected using an excitation wavelength of 490 nm with slit widths of 3 nm and 6 nm and a quartz cuvette (1 cm path length). The fluorescence intensity at 600 nm increased as the concentration of **14** increased from 0 to 100 mol%. When the concentration of **14** was in excess of 100 mol%, the intensity remained constant. Plotting and curve fitting of the fluorescence intensity (I) at 600 nm against the concentration (c) of **14** ranging from 0 to 100 mol% gave a polynomial equation ($I = -47072(c)^2 + 154201(c) + 204014$) with $R^2 = 0.99603$.

Figure S12. Fluorescence spectra of the complexes formed from 1, Et_2Zn and varying concentrations of 14 from 0-100 mol% (blue) and 120-200 mol% (red).

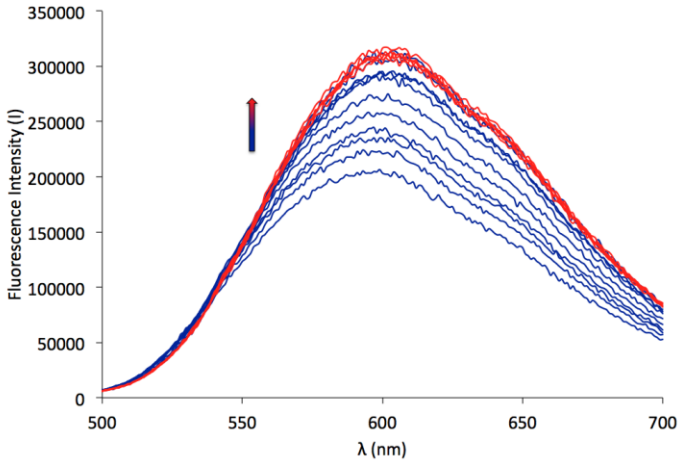

Figure S13. Fluorescence intensity (I) measured at 600 nm plotted against ratio of [14]/[1].

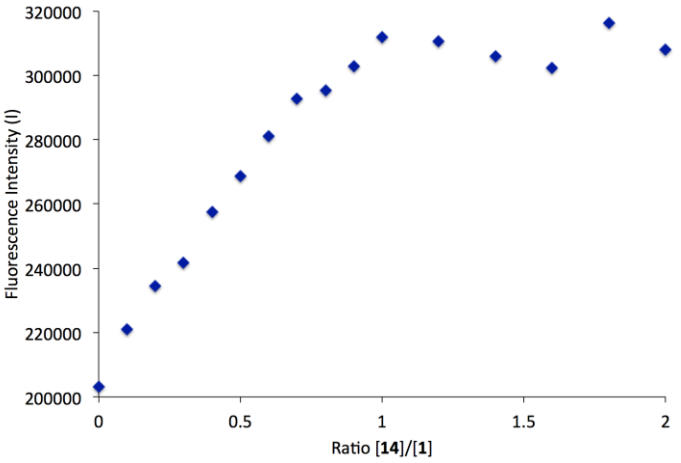

Figure S14. Curve fitting of the fluorescence emission at 600 nm.

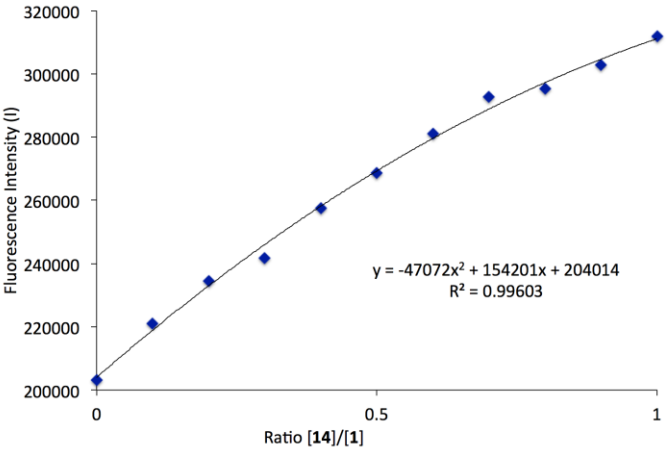

Five solutions of **1** were prepared and added to solutions of varying concentrations of **14** as described above. Using the regression equations and the measured fluorescence intensity at 600 nm, the concentration of these samples was determined with high accuracy.

Table S2. Experimentally determined concentrations of five samples of varying concentration of 14 using the fluorescence response at 600 nm.

Actual Concentration (mM)	Calculated Concentration (mM)
0.56	0.60
1.01	1.09
2.36	2.29
2.93	2.96
3.34	3.38

4.3. Ee determination of hydrobenzoin 25

CD responses of the Ti complex prepared from **1** and **25** were analyzed using stock solutions of **1** (0.00375 M in THF) and **25** (0.07 M in THF) with varying enantiomeric composition (+100, +80, +60, +40, +20, 0, -20, -40, -60, -80, -100 ee). To these solutions was added Ti(O*i*-Pr)$_4$ (2.6 µL, 0.0013 mmol, 0.5 M in THF). After 15 minutes, CD analysis was carried out as described above at 1.13 x 10^{-4} M in anhydrous diethyl ether. The Cotton effect amplitudes at 375 and 470 nm were plotted against the enantiomeric excess of **25**.

Figure S15. CD Spectra of the Ti complex obtained with 1 and scalemic samples of 25.

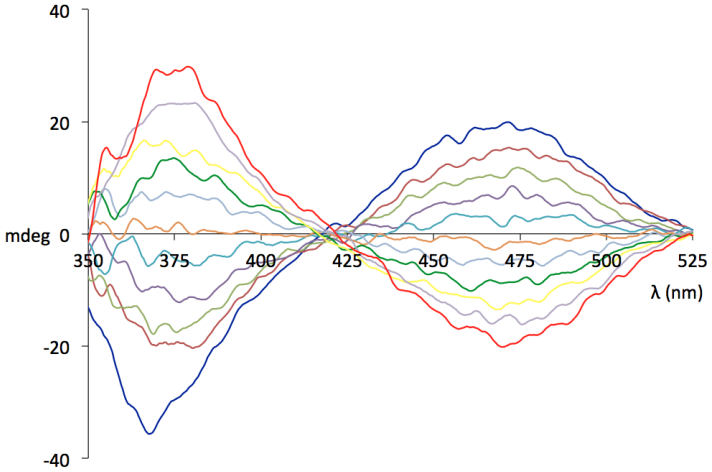

Figure S16. Linear relationship between the CD amplitudes at 375 nm (red) and 470 nm (blue) and the enantiomeric excess of 25.

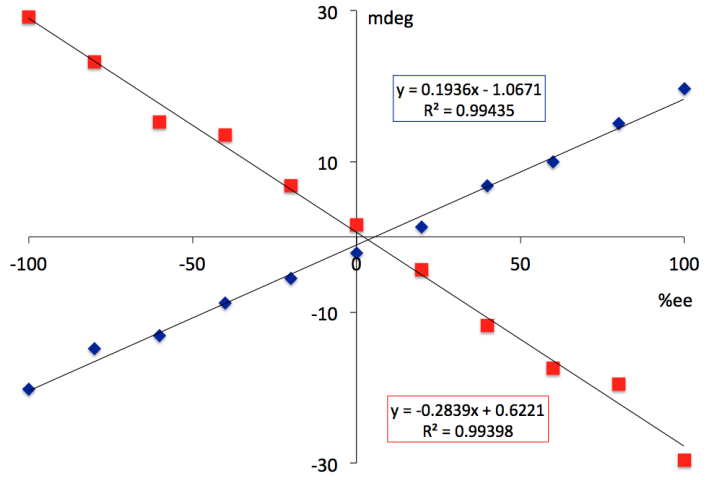

Five scalemic samples of **25** were prepared and subjected to CD analysis with **1** and Ti(O*i*-Pr)$_4$ as described above. Using the regression equations obtained above and CD amplitudes measured at 375 and 470 nm, the enantiomeric excess of these samples was determined (Table 3).

Table S3. Ee determination of hydrobenzoin.

Actual % ee (1*R*,2*R*)	Calculated % ee at 375 nm (*1R*,2*R*)	Calculated % ee at 470 nm (1*R*,2*R*)	Average % ee
76.0	79.7	79.3	79.5
68.0	70.5	66.9	68.7
12.0	13.6	12.6	13.1
-26.0	-24.2	-22.3	-23.3
-89.0	-91.3	-86.8	-89.1

4.4. Determination of the concentration of 25

The change in the fluorescence of the complex between **1** and Ti(O*i*-Pr)$_4$ upon addition of **25** was analyzed using samples containing various amounts of **25**. First, 350 µL solutions of **1** (0.00375 M in THF) were placed in 13 vials. To each vial was then transferred a solution of **25** (0.07 M in THF) in varying amounts (0, 10, 20, 30, 40, 50, 60, 70, 80, 90, 100, 120, 140, and 160 mol%). Ti(O*i*-Pr)$_4$ (2.6 µL, 0.0013 mmol, 0.5 M in THF) was added to each vial and the mixtures were allowed to react for 15 minutes. Fluorescence spectra were collected as described above. The fluorescence intensity at 585 nm increased as the concentration of **25** increased from 0 to 100 mol%. When the concentration of **25** was in excess of 100 mol%, the intensity remained constant. Plotting and curve fitting of the fluorescence intensity (I) at 585 nm against the concentration (c) of **25** ranging from 0 to 100 mol% gave a polynomial equation ($I = -584891(c)^3 + 777014(c)^2 + 548022(c) + 254088$) with $R^2 = 0.99401$.

Figure S17. Fluorescence spectra of the complexes formed from 1, Ti(O*i*-Pr)$_4$ and varying concentrations of 25 from 0-100 mol% (blue) and 120-160 mol% (red).

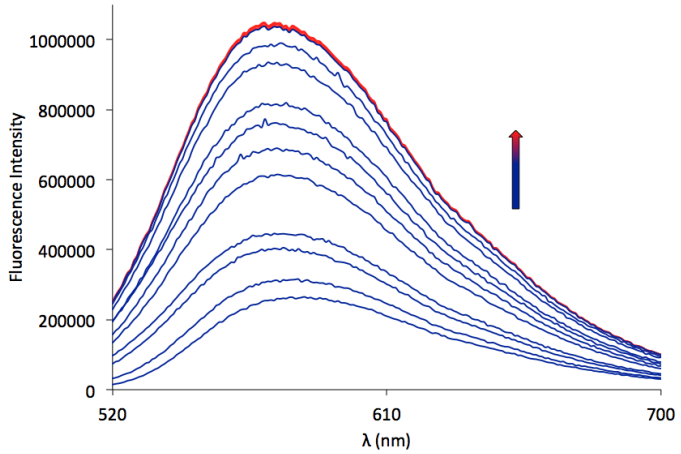

Figure S18. Fluorescence intensity (I) measured at 585 nm plotted against ratio of [25]/[1].

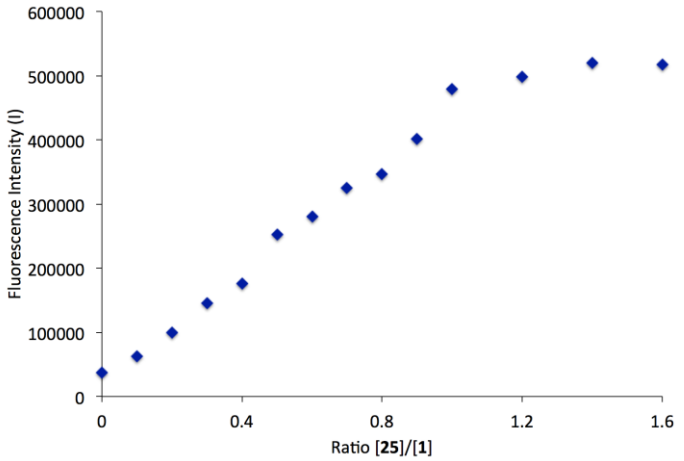

Figure S19. Curve fitting of the fluorescence emission at 585 nm.

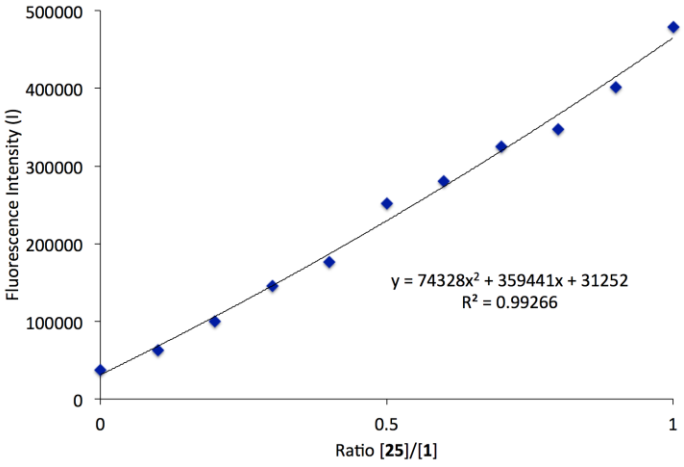

Five solutions of **1** were prepared and added to solutions of varying concentrations of **25** as described above. The concentration of these samples was determined with high accuracy using the regression equation obtained above and the measured fluorescence intensity at 585 nm.

Table S4. Experimentally determined concentrations of five samples of varying concentration of 25 using the fluorescence response at 600 nm.

Actual Concentration (mM)	Calculated Concentration (mM)
0.56	0.53
1.01	1.01
1.76	1.88
2.36	2.47
2.93	2.72

5. Ee and concentration analysis of hydrobenzoin 25 obtained by asymmetric Sharpless dihydroxylation

Figure S20. Asymmetric Sharpless dihydroxylation of *trans*-stilbene.

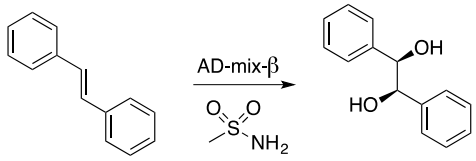

The efficacy of **1** for the determination of both concentration and ee was tested using the asymmetric Sharpless dihydroxylation as an example. Solutions of **1** (1.57 mg, 0.005 mmol) and the crude product obtained as described above (1.07 mg) in 0.5 mL of THF were prepared and treated with Ti(O*i*-Pr)$_4$ (1.48 μL, 0.005 mmol). A fluorescence spectrum was obtained via the method described in section 4.4 at a concentration of 1.14 x 10^{-4} M, and the concentration was calculated using the regression equation obtained in section 4.4. Then, a CD spectrum was obtained at 1.14 x 10^{-4} M as described in section 4.3. The Cotton effect intensity (mdeg) was normalized for the concentration calculated by the fluorescence analysis using the relative mol% (χ) of hydrobenzoin as shown in equations 1 (470 nm) and 2 (375 nm). This value was then applied in the linear regression equations obtained in Section 4.3 to determine the enantiomeric excess based on the average values at 470 and 375 nm (equations 1 and 2, respectively). Importantly, it was not necessary to obtain new calibration curves which systematically simplifies the sensing analysis.

Equation 1

$$ee = \frac{\frac{mdeg}{X} + 1.0671}{0.1936}$$

Equation 2

$$ee = \frac{\frac{mdeg}{X} - 0.6221}{-0.2839}$$

Table S5. Comparison of calculated and actual ee and concentration values of hydrobenzoin obtained by asymmetric Sharpless dihydroxylation.

		Conventional Analysis		Sensing Results			
Entry	**Temp.**	**Isolated Yield (%)**	**% ee (*R*,*R*) by HPLC**	**Calculated Yield (%)**	**% ee at 470 nm (*R*,*R*)**	**% ee at 375 nm (*R*,*R*)**	**Average % ee**
AD-mix-β	0 °C	99.1	99.1	95.4	98.2	99.6	98.9
AD-mix-β	25 °C	71.0	86.3	65.3	85.5	90.0	87.7
AD-mix-β	50 °C	17.7	75.4	12.2	73.8	77.8	75.8
Cinchonine	25 °C	54.2	0.0	51.1	2.1	0.5	1.3

Overall, the use of ligand **1** with Ti(O*i*-Pr)$_4$ as chemosensor for the determination of ee and concentration of hydrobenzoin requires far less time and solvent than column chromatography and HPLC analysis. Because both spectroscopic measurements were obtained at the same concentration, one sample is sufficient to obtain reaction yield and ee using a total of 2.5 mL of solvent. Comparatively, purification of the crude reaction mixture by flash chromatography requires ~380 mL solvent, and HPLC analysis requires 25-30 mL. The spectroscopic measurements are also time efficient, with each measurement requiring ~15 seconds, while HPLC requires 25-30 minutes to completely separate the two enantiomers.

Figure S21. HPLC separation of the product obtained with AD-mix-β at 0 °C on a Chiralcel OJ column using hexanes:*i*-PrOH (92:8 v/v) as mobile phase.

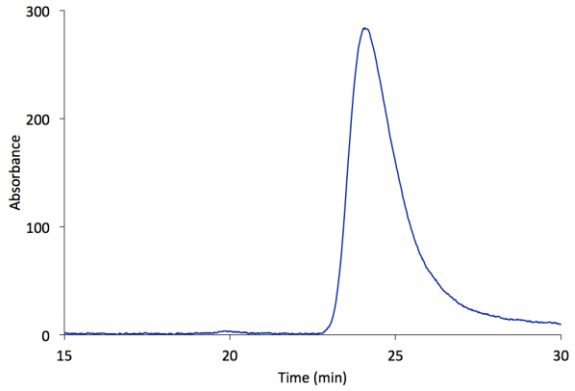

Figure S22. HPLC separation of the product obtained with AD-mix-β at 25 °C on a Chiralcel OJ column using hexanes:*i*-PrOH (92:8 v/v) as mobile phase.

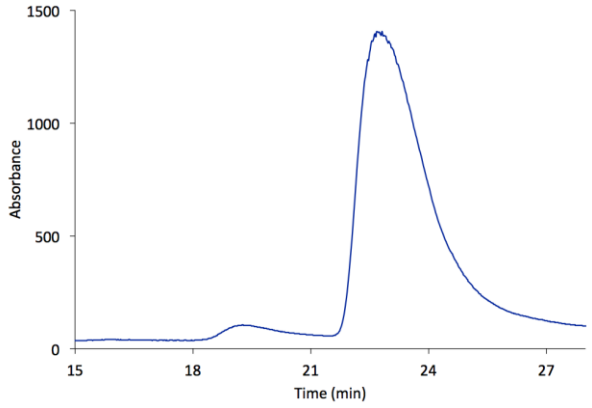

Figure S23. HPLC separation of the product obtained with AD-mix-β at 50 °C on a Chiralcel OJ column using hexanes:*i*-PrOH (92:8 v/v) as mobile phase.

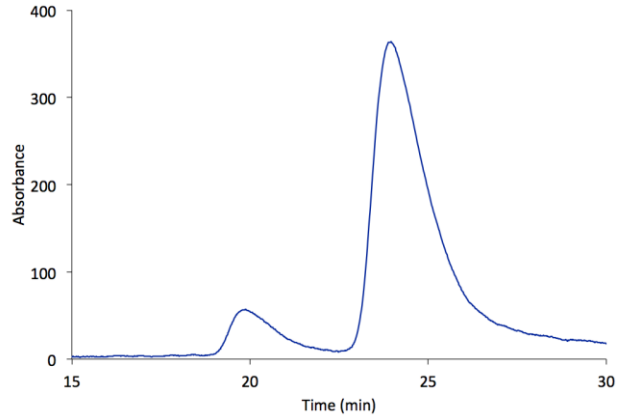

Figure S24. HPLC separation of the product obtained with cinchonine at 25 °C on a Chiralcel OJ column using hexanes:*i*-PrOH (92:8 v/v) as mobile phase.

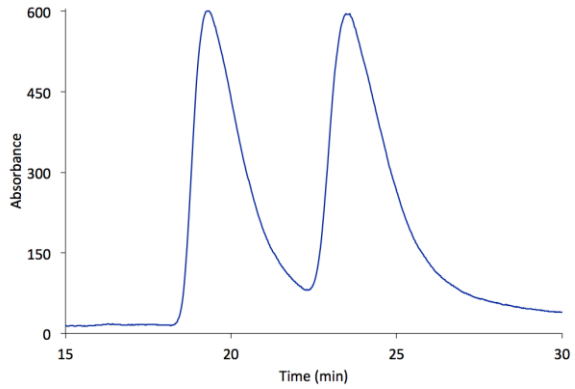

6. MS Analysis of the in-situ complex formation

A solution of **1** (1.57 mg, 0.005 mmol) and **4** (0.90 mg, 0.005 mmol) in 1 mL of a dry THF:MeOH mixture (1:1 v/v) was prepared. Then, Et_2Zn (5 µl, 0.005 mmol, 1M in hexanes) was added and the mixture was stirred for 10 minutes. Electrospray mass spectrometry (positive ion mode) showed the presence of a bimetallic complex containing 2 equivalents of **1, 4** and Zn.

Figure S25. MS Spectrum of the complex obtained from 1, Et_2Zn and (1*R*,2*R*)-4.

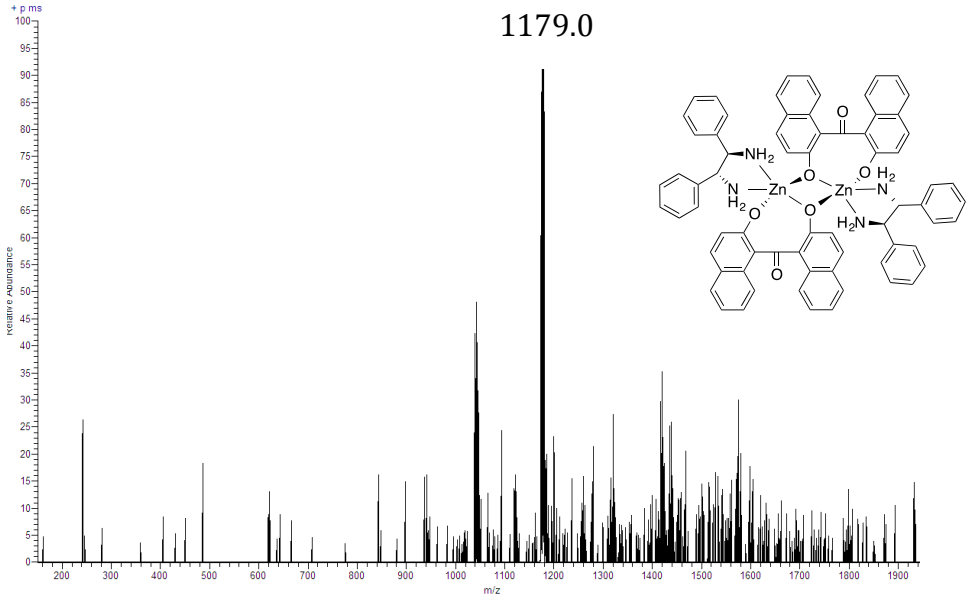

ESI-MS: m/z = 1179.0 (M^{+1})

A solution of **1** (1.57 mg, 0.005 mmol) and **10** (0.90 mg, 0.005 mmol) in 1 mL of a dry THF:MeOH mixture (1:1 v/v) was prepared. Then, Et_2Zn (5 µl, 0.005 mmol, 1M in hexanes) was added and the mixture was stirred for 10 minutes. Electrospray mass spectrometry (positive ion mode) showed the presence of a bimetallic complex containing 2 equivalents of **1, 10** and Zn.

Figure S26. MS Spectrum of the complex obtained from 1, Et_2Zn and (1*R*,2*S*)-10.

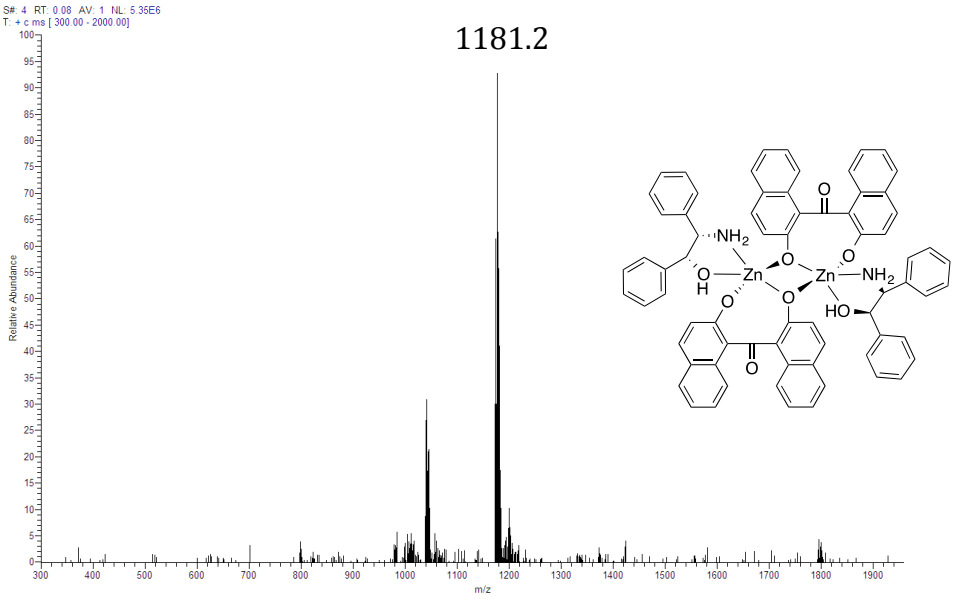

ESI-MS: m/z = 1181.2 (M^{+1})

A solution of **1** (1.57 mg, 0.005 mmol) and **14** (0.90 mg, 0.005 mmol) in 1 mL of a dry THF:MeOH mixture (1:1 v/v) was prepared. Then, Et_2Zn (5 µl, 0.005 mmol, 1M in hexanes) was added and the mixture was stirred for 10 minutes. Electrospray mass spectrometry (positive ion mode) showed the presence of a bimetallic complex containing 2 equivalents of **1, 14** and Zn.

Figure S27. MS Spectrum of the complex obtained from 1, Et_2Zn and (1*R*,2*S*)-14.

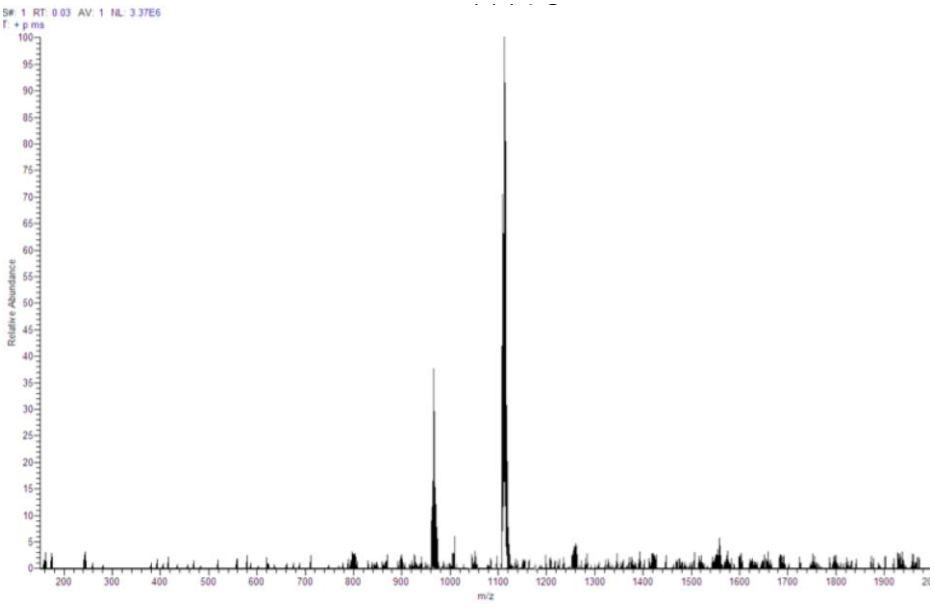

ESI-MS: m/z = 1114.8 (M^{+1})

A mixture of **1** (1.57 mg, 0.005 mmol) and Me_3Al (2.5 µl, 0.005 mmol, 2M in hexanes) was stirred in a THF:MeOH mixture (1:1 v/v) for 10 minutes. To this solution was added **23** (0.76 mg, 0.005 mmol) and the mixture was subjected to ESI-MS analysis. A complex containing 2 equivalents of **1**, Al, and **23** was observed.

Figure S28. MS Spectrum of the complex obtained from 1, Me_3Al and (*R*)-23.

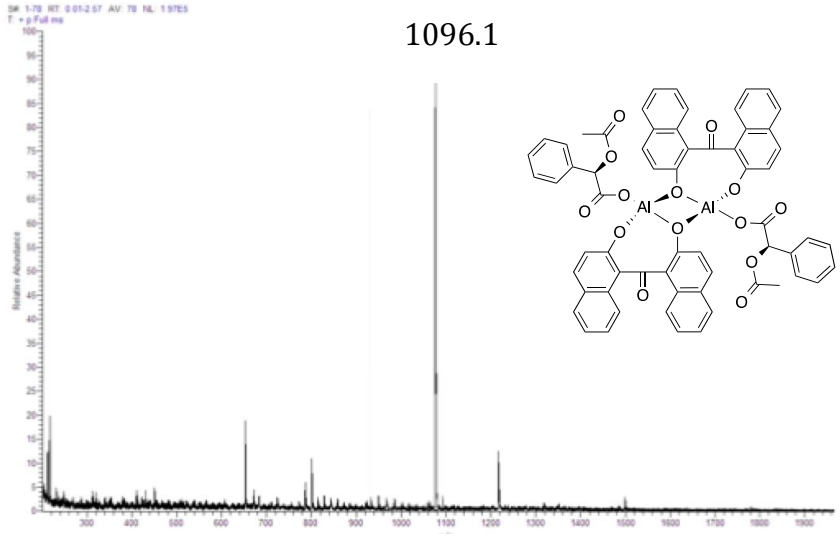

ESI-MS: m/z = 1096.1 (M^{+1})

A solution of **1** (1.57 mg, 0.005 mmol) and **25** (1.07 mg, 0.005 mmol) in 1 mL of a dry $CHCl_3$:THF mixture (3:1 v/v) was prepared. Then, Ti(O*i*-Pr)$_4$ (1.5 µl, 0.005 mmol) was added and the mixture was stirred for 10 minutes. Electrospray mass spectrometry (positive ion mode) showed the presence of a bimetallic complex containing 2 equivalents of **1, 25,** Ti and 1 equivalent of isopropyl alcohol.

Figure S29. MS Spectrum of the complex obtained from 1, Ti(O*i*-Pr)$_4$ and (1*R*,2*R*)-25.

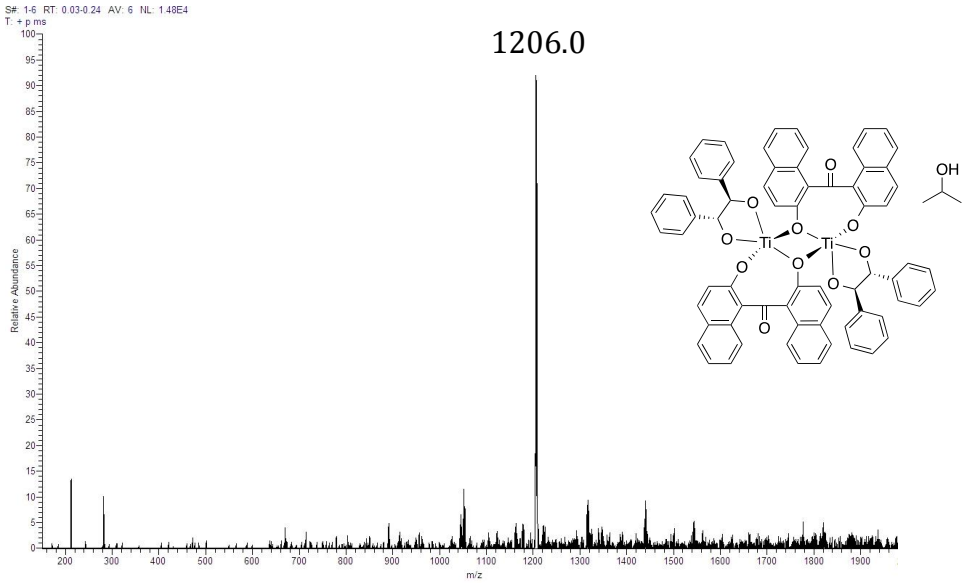

ESI-MS: m/z = 1206.0 (M^{+1}) (2:2:2 + isopropyl alcohol)

7. Analysis of the sensing mechanism with the stereodynamic Ti complex

An MS study was performed to investigate the preference for the homochiral vs the heterochiral species of the dinuclear Ti complex formed from **1**, Ti(O*i*-Pr)$_4$ and either **25** or **26**. A solution containing (2*R*,3*R*)-**26** with **1** and Ti(O*i*-Pr)$_4$ was prepared as described above. Then, 1 equivalent of (1*S*,2*S*)-**25** was added and the mixture was allowed to equilibrate for 5 minutes. The resulting MS spectrum showed a mixture of [**1**-Ti-**26**]$_2$ with a molecule of isopropyl alcohol as well as [**1**-Ti-**25**]$_2$ with a molecule of isopropyl alcohol. No sign of the heterochiral complex was observed.

Figure S30. MS Spectrum of the complexes obtained from 1, Ti(O*i*-Pr)$_4$ and a mixture of (1*S*,2*S*)-25 and (2*R*,3*R*)-26.

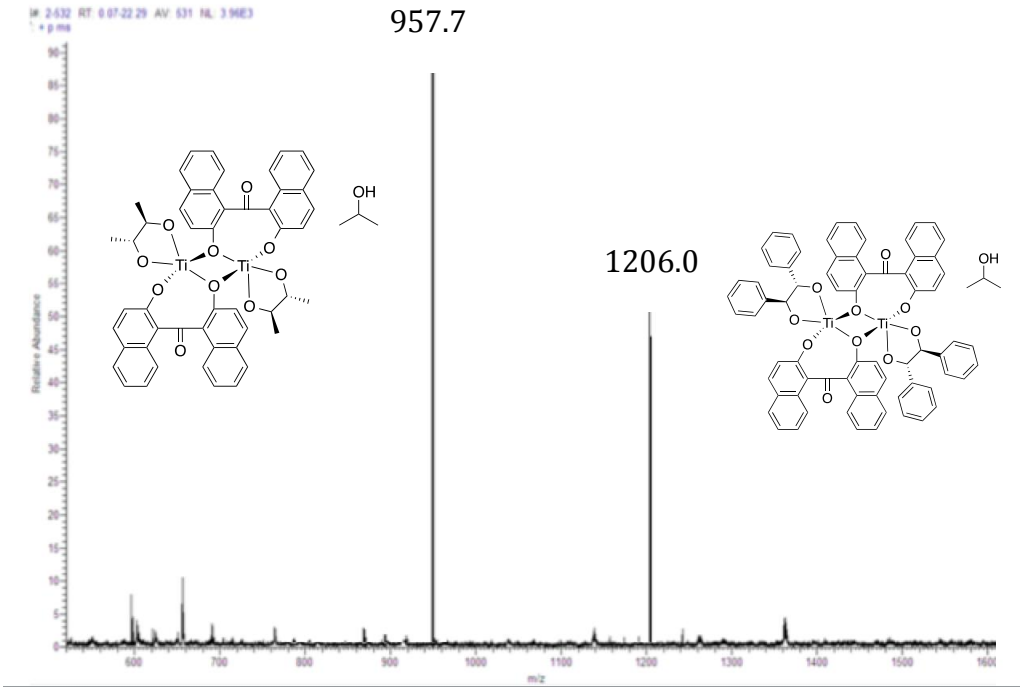

ESI-MS: [**1**-Ti-**26**]$_2$ m/z = 957.7 (2:2:2 + isopropyl alcohol); [**1**-Ti-**25**]$_2$ m/z = 1206.0 (2:2:2 + isopropyl alcohol)

A solution containing (1*S*,2*S*)-**25** with **1** and Ti(O*i*-Pr)$_4$ was prepared as described above. Then, 1 equivalent of (2*S*,3*S*)-**26** was added and MS was collected immediately. The resulting MS spectrum showed a mixture of [**1**-Ti-**25**]$_2$ with a molecule of isopropyl alcohol, as well as a mixed species consisting of a bimetallic titanium complex with two molecules of **1**, one molecule of **25**, and one molecule of **26** and one equivalent of isopropyl alcohol.

Figure S31. MS Spectrum of the complexes obtained from 1, Ti(O*i*-Pr)$_4$, (1*S*,2*S*)-25, and (2*S*,3*S*)-26.

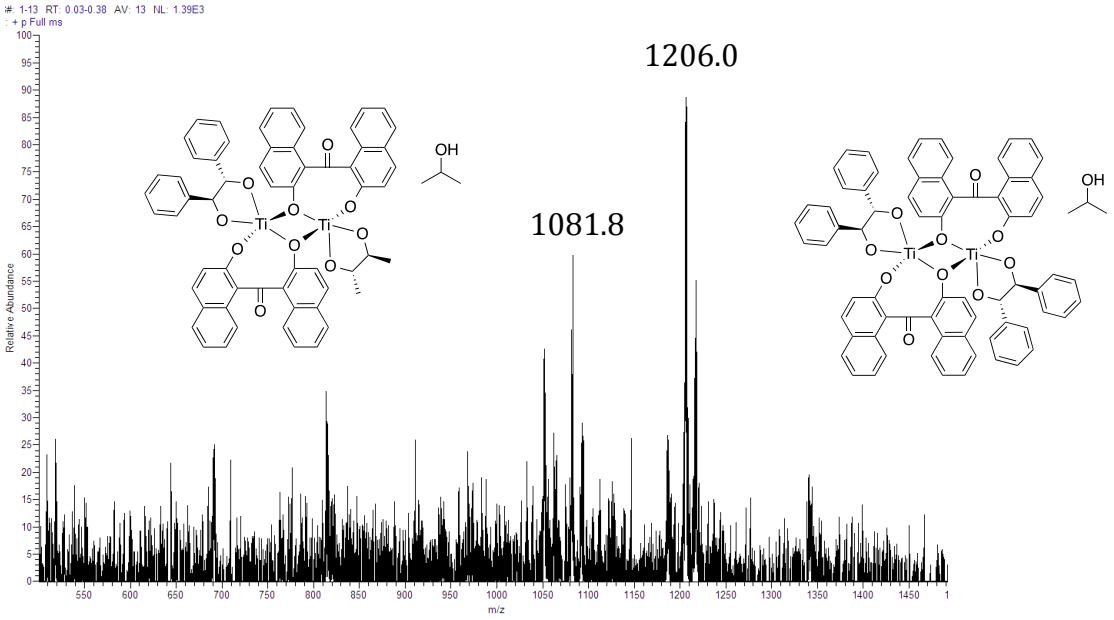

ESI-MS: [**1**-Ti-**25**]$_2$ m/z = 1206.0 (2:2:2 + isopropyl alcohol); [**1**$_2$-Ti$_2$-**25**-**26**] m/z = 1081.8 (2:2:1:1 + isopropyl alcohol)

The displacement of the isopropyl units from Ti was monitored by ^{1}H NMR. The septet representing the tertiary proton of the isopropyl alkoxide bound to Ti is centered at 4.47 ppm in $CDCl_3$. When one equivalent of **1** was added, a new septet appeared at 4.01 ppm and was present in a 1:1 ratio with the original septet, indicating that two isopropyl alcohol units were displaced by the ligand as expected. Then, one equivalent of **25** was added and the remaining isopropoxides were displaced as evidenced by the disappearance of the septet at 4.47 ppm with the septet at 4.01 ppm remaining. The aromatic region showed line broadening at room temperature and at -60 °C.

Figure S32. Excerpt of the NMR spectrum showing the methine proton septet in [Ti(O*i*-Pr)$_4$] (red), after addition of one equivalent of 1 (green), and upon addition of one equivalent of 25 (blue).

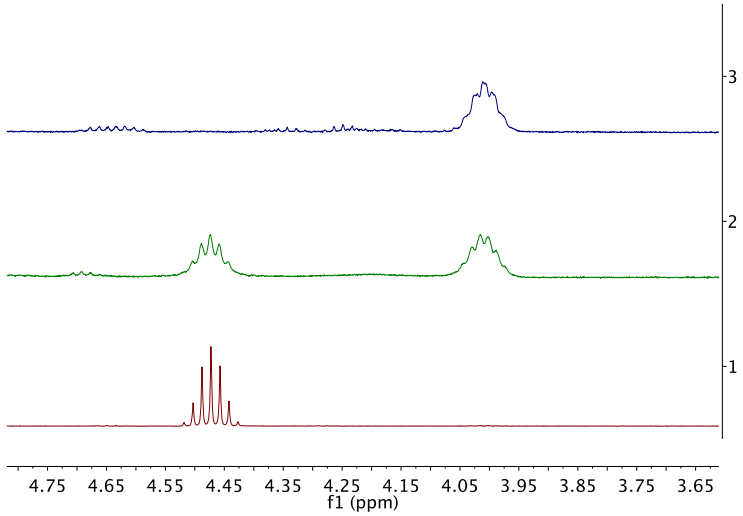

A similar change was observed for the methyl doublet, which is centered at 1.23 ppm for Ti(O*i*-Pr)$_4$. As above, when one equivalent of **1** was added, a new doublet appeared centered at 1.19 ppm with a ratio of 1:1 with the original doublet. Upon addition of **25**, the original methyl doublet nearly disappeared, while the new doublet remained.

Figure S33. Excerpt of the NMR spectrum showing the methyl doublet of [Ti(O*i*-Pr)$_4$] (red), after addition of one equivalent of 1 (green), and upon addition of one equivalent of 25 (blue).

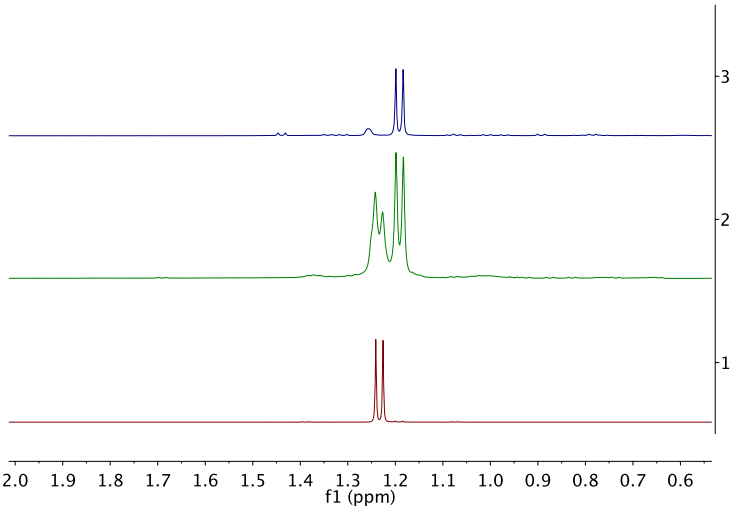

A solution of **1** was prepared as described in section 3 and 0.5 mL portions were placed in 4 mL vials. Then, varying molar ratios of **25** were added (0.25, 0.5, 0.75, 1.0, 1.5, 2.0) and CD spectra were collected upon addition of Ti(O*i*-Pr)$_4$. The CD intensity at 375 nm and 470 nm were plotted vs the molar ratio of [**25**]/[**1**]. The CD signal increased from 0-1 equivalent, then did not significantly change upon addition of excess **25**.

Figure S34. CD intensity at 375 nm (triangle) and 470 nm (diamond) for the complex obtained from Ti(O*i*-Pr)$_4$, 1, and (1*R*,2*R*)-25 (blue) and for (1*S*,2*S*)-25 (red).

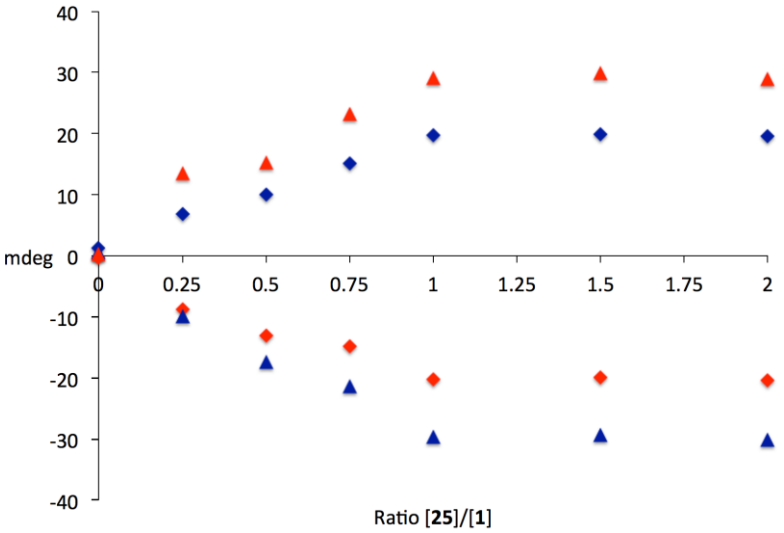

8. Crystallography

A single crystal of compound **3** was obtained by slow evaporation of a concentrated chloroform solution. Crystallographic analysis was performed at 100 K using a Siemens platform diffractometer with graphite monochromated Mo-Kα radiation (λ = 0.71073 Å). Data were integrated and corrected using the Apex 2 program. The structure was solved by direct methods and refined with full-matrix least-square analysis using SHELX-97-2 software. Non-hydrogen atoms were refined with anisotropic displacement parameters. The asymmetric unit contains one molecule of **3**. Crystal structure data: Formula $C_{23}H_{18}O_3$, M = 342.37, crystal dimensions 0.4 x 0.2 x 0.1 mm, monoclinic, space group C2/c, *a* = 26.52 Å, *b* = 8.52 Å, *c* = 18.28 Å, α = 90.0°, β = 125.72°, γ = 90.0°, V = 3359.47 Å^3, Z = 8, ρ_{calcd} = 1.354 g cm^{-3}.

Figure S35. X-Ray structure of bis(2-methoxy-1-naphthyl)ketone, 3.

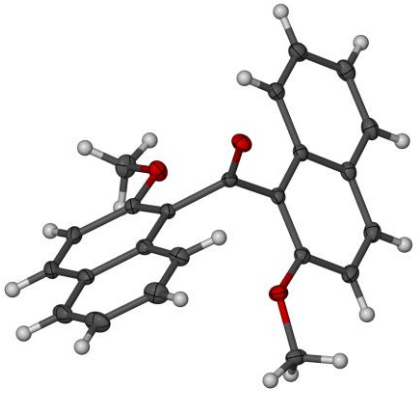

A single crystal of compound **1** was obtained by slow evaporation of a concentrated chloroform solution. Crystallographic analysis was performed with identical parameters as listed above. The asymmetric unit contains one molecule of **1**. Crystal structure data: Formula $C_{21}H_{14}O_3$, M = 314.32, crystal dimensions 0.5 x 0.2 x 0.1 mm, orthorhombic, space group $P2_12_12_1$, *a* = 7.4826(5) Å, *b* = 13.4485(8) Å, *c* = 14.9052(9) Å, α = 90.0°, β = 90.0°, γ = 90.0°, V = 1499.91(16) $Å^3$, Z = 4, ρ_{calcd} = 1.392 g cm^{-3}.

Figure S36. X-Ray structure of bis(2-hydroxy-1-naphthyl)ketone, 1